# HAMILTONIAN GRAPH REPRESENTATION OF ZEOLITE FRAMEWORKS AND Si, Al ORDERING IN THE FRAMEWORK

M. SATO
*Department of Applied Chemistry, Gunma University, Kiryu, Gunma, Japan*

## Abstract

In the first part, a topological characterization of various zeolite frameworks is performed on the basis of the Hamiltonian graph. It affords a simple representation of the framework connectivity, and presents some possibility of the classification as well as the prediction of unknown frameworks. In the second part, a simple and direct method based on the connectivity matrix is presented, by which all the possible Al distributions in a given framework are derived exhaustively under the restriction of Loewenstein's rule. An example of Al preference site determination is applied for zeolite ZSM-5 and compared with the result by the SCF-MO method.

## 1. Introduction

Microporous zeolite frameworks are constructed from interlinking $SiO_4$ and $AlO_4$ tetrahedra to form channels and cavities in which relevant ion exchangeable or catalytic activity and selectivity are performed. The physical and chemical properties of zeolites depend not only on the topological characteristics of the framework, but also on the Si, Al distribution in the framework. The main current topics in zeolite structural chemistry are, therefore, to clarify the principle of framework construction as well as the extent of the framework effect on the Si, Al distribution. In this paper, some graph-theoretical approaches have been introduced to develop the problems.

## 2. Hamiltonian graph representation of zeolite frameworks

As mentioned above, the diversity of zeolite frameworks depends on that of the geometrical connectivity of constituting $TO_4$ tetrahedra. In order to clarify the topological characteristics of the frameworks, several concepts have been presented to date:

(1) Secondary building unit (SBU) [1].
(2) Loop configuration (LCG) [2].
(3) Concentric cluster (CCL) [3].
(4) Coordination sequence (CSQ) [4].
(5) Coordination degree sequence (CDS) [3].

Here, (1), (2), and (3) concern the graphical representation of the framework characteristics, while (4) and (5) concern their mathematical quantifications. The SBU concept is a simple and effective geoemetrical means of characterizing the complicated zeolite frameworks, and a total of sixteen SBUs are now available [5]. The LCG concept concerns the configuration of 4-membered rings around a given node site. The LCG can be completely incorporated into the CCL concept, which was formerly presented as the Coordination Network [6,7]. These graphical representations aim at representing the framework characteristics in terms of constituent basic units or clusters, but no satisfactory results have as yet been presented.

As is well known, zeolite frameworks are in a crystalline state, which means the framework is constituted of unit cells arranged in a given translational symmetry. Therefore, it is fully expected that basic structural characteristics are condensed on the node connectivity in the unit cell.

Figure 1(a) shows a simple 3-connected network of carbon graphite. The unit cell contains two carbon atoms designated by *a* and *b*. An *a* is connected with three *b*'s, while a *b* is connected with three *a*'s. Thus, their connectivity can be simply represented graphically as in fig. 1(b). Figure 2(a) shows a 4-connected framework of cristobalite $SiO_2$, one of the silica polymorphs. This compound contains four Si atoms in the unit cell designated by *a*, *b*, *c* and *d*. An *a* is connected with two *b*'s and two *d*'s, a *b* with two *a*'s and two *c*'s, and so on. Their connectivities are shown in fig. 2(b). A more complex example of a sodalite zeolite framework is shown in fig. 3(a), and its graphical representation in fig. 3(b). Figure 4(a) shows a framework of zeolite A containing 24 nodes in the unit cell, and its graphical representation is given in fig. 4(b). It is interesting to note that all these graphs have a cycle which contains all the nodes in the unit cell. This means that the graph is Hamiltonian [8]. At the present time, we cannot conclude that all the 4-connected frameworks are Hamiltonian, but most of the real zeolite frameworks, including both natural and synthetic ones, have proved to be Hamiltonian, although tests have been run only for frameworks with the maximum node number 36 in the unit cell. Various patterns which appear in the graph reflect the connectivities between them, but it must be noted that the graph sometimes shows unexpected patterns, such as 4-membered rings in the cristobalite framework (fig. 2(b)) or triple bonds in the graphite one (fig. 1(a)), all of which cannot be expected in their real frameworks. These are obviously due to the restriction of translational symmetry. If we extend the unit cell size appropriately, the unfavorable patterns would be eliminated to disclose the real 6-membered rings or the single bonds.

Anyway, a given framework can be represented in terms of a corresponding Hamiltonian graph. Therefore, structural correlations between the frameworks can now be readily drawn on the basis of these Hamiltonian graphs. At this point, it is necessary to clarify the construction principle of the Hamiltonian graphs and correlate them with each other.

In the 4-connected frameworks, each node has four bonds, two of which are used for the construction of the Hamiltonian path, and the other two for the construction

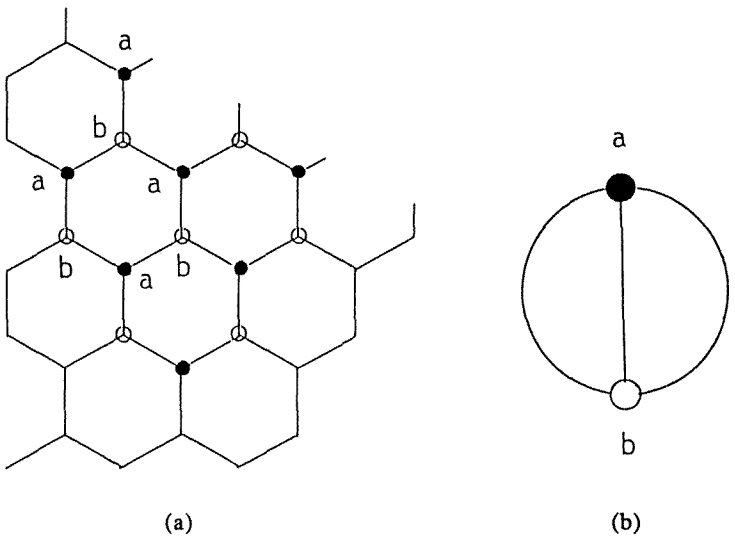


Fig. 1. (a) Carbon graphite network, and (b) its graphical representation.

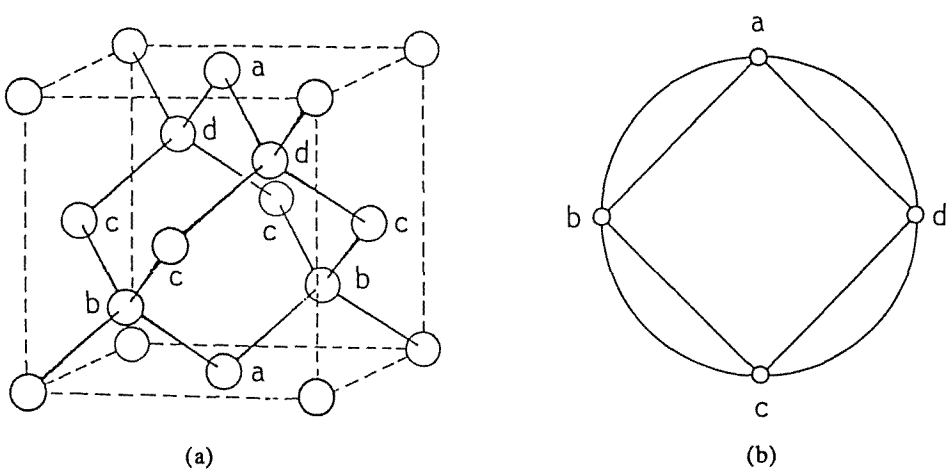


Fig. 2. (a) Cristobalite $SiO_2$ framework, in which oxygen atoms are omitted, and (b) its graphical representation.

of the framework. From the fact that a framework edge is formed by a connection of two bonds, it can be easily proved that the total number of framework edges except for the Hamiltonian path becomes the number of nodes $P$. Therefore, the possible number of Hamiltonian graphs is determined by the number of different distributions of the $P$ framework edges over the $P$ nodes. In their derivation, we first notice that the graph aimed at is regular of degree 2, and therefore every component is a cycle [8]. This means that the graph can be represented

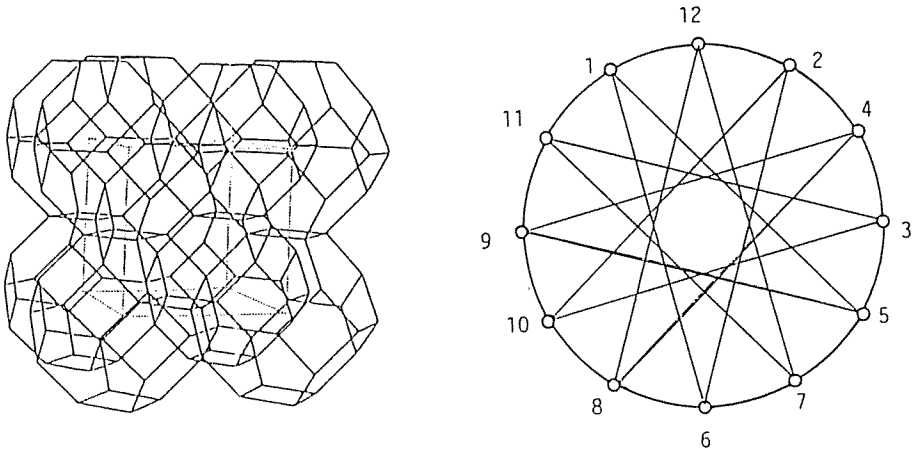


(a) (b)

Fig. 3. (a) Sodalite framework, and (b) its graphical representation.

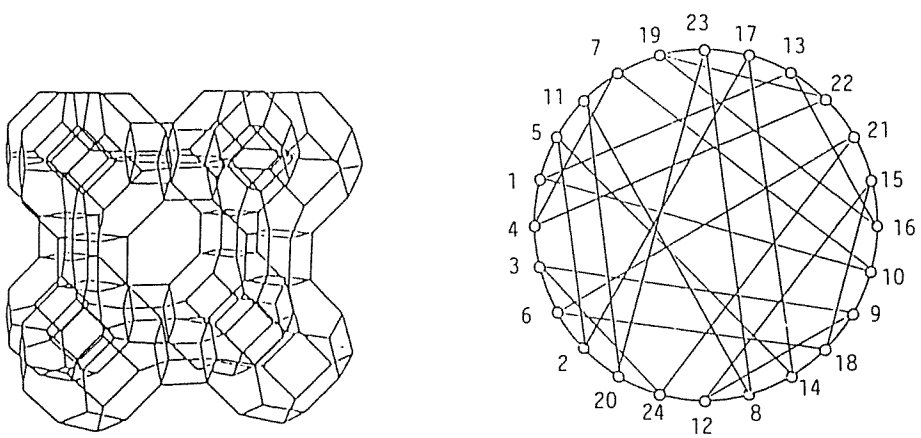


(a) (b)

Fig. 4. (a) Zeolite A framework, and (b) its graphical representation.

by a simple permutation notation (12)(345) or (12)(354), as shown in fig. 5. Similarly, the Hamiltonian graph of the sodalite framework in fig. 3(b) can be represented as (1,5,9,4,8,12,7,11,3,10,2,6), and that of zeolite A in fig. 4(b) as (1,10,7,4,22,19,16,13)(3,9,12,15,18,6,21,24)(2,5,14,17)(8,11,20,23). Thus, the distributions of edges can be performed mathematically on the basis of the permutation operations. Some examples for $P$ = 3, 4 and 5 are shown in fig. 6. In the case of $P$=3, we have only one kind of Hamiltonian graph. This is exactly the type of

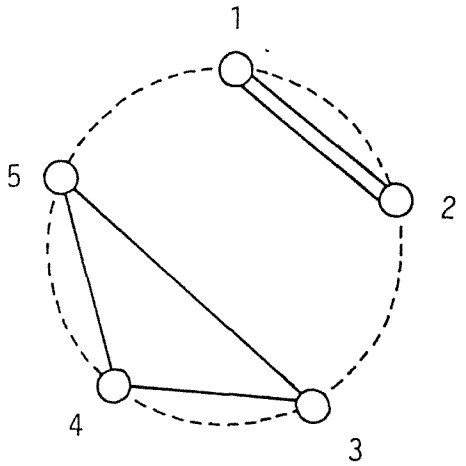


Fig. 5. Hamiltonian graph notation by a permutation notation (12)(345).

quartz, one of the silica polymorphs, $SiO_2$. In the case of $P = 4$, we have four kinds. Two of them are the types of cristobalite (4–3) and tridymite (4–1), which are also well-known silica polymorphs. The existence of the remaining two types (4–2, 4–4) is not as yet known. In the case of $P = 5$, we have six kinds of Hamiltonian graphs, none of which are yet known as the real structure. The Hamiltonian graphs obtained can be classified on the basis of their permutation configuration. For example, both 5–1 and 5–2 in fig. 6 contain two permutation cycles such as (12)(345), while 5–3, 5–4 and 5–5 contain one permutation cycle such as (12345), from which they can be easily classified into two groups.

As shown here, the Hamiltonian graph is useful not only for a simple representation of complex connectivity, but also for prediction as well as classification of zeolite frameworks. As will be shown in the next section, this also serves for characterizing the Al distribution in the frameworks.

## 3. Determination of Si, Al distribution in zeolite frameworks

The Si, Al distribution in zeolite frameworks cannot be uniquely determined by the X-ray diffraction method, because their X-ray scattering powers are nearly the same. However, their local ordering can now be precisely determined by solid state $^{29}Si$ MAS NMR spectroscopy. One of the distinguished results is a confirmation of the validity of Loewenstein's rule, that is, the avoidance rule of an Al–Al pair in the first neighbor. On the basis of these data, various long-range ordering models have been presented and correlated with the physical and chemical

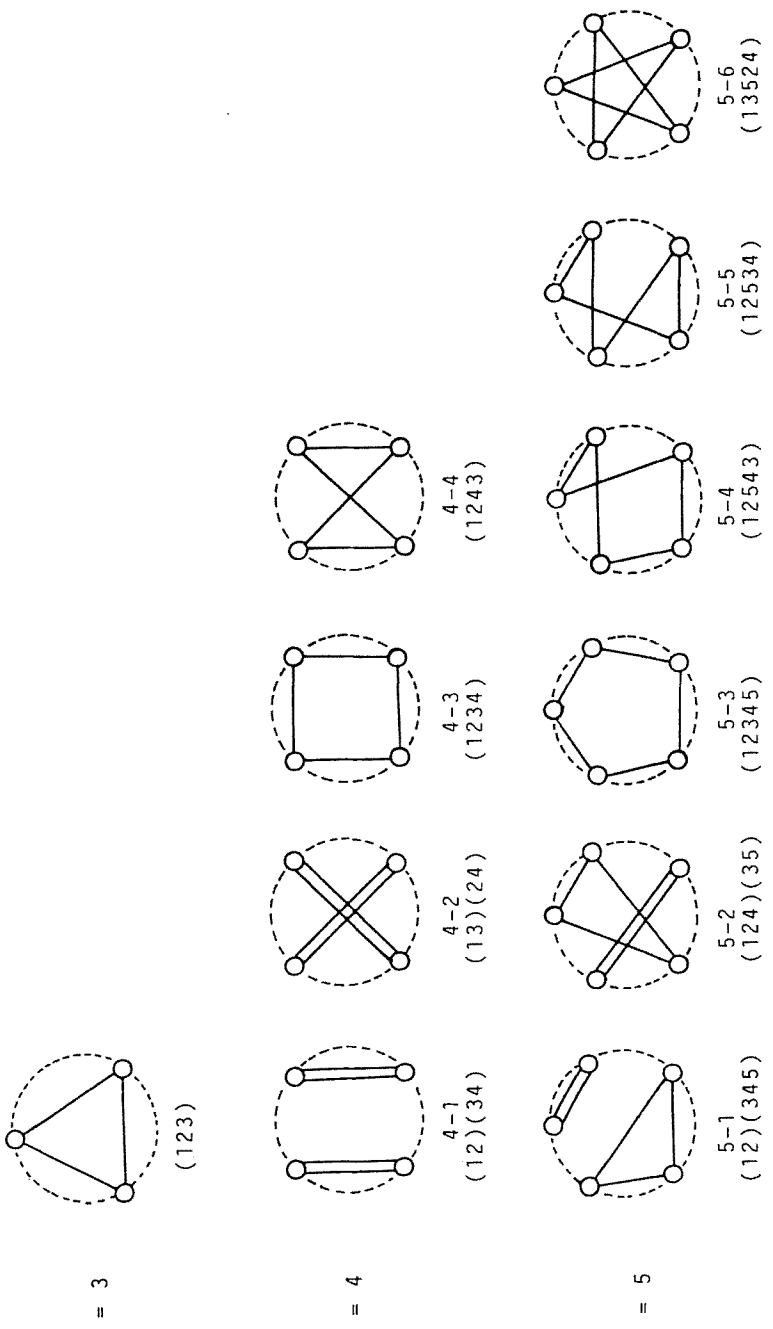


Fig. 6. Possible Hamiltonian graphs for $P = 3$, 4 and 5, and their permutation notations.

properties [9–14]. On the other hand, more strict quantum chemical studies have been performed to determine the Al sites in the framework [15–24]. If the nodes involved are small in number, this can be easily done, but as the number increases, it becomes very difficult to complete. In this paper, a simple and complete method based on the connectivity matrix is introduced, by which all possible distributions can be exhaustively derived. In the following, we make only two simple assumptions.

(1) The translational symmetry inherent to the zeolite framework also holds in the Si, Al distribution. This means the distribution can be treated within a given unit cell.

(2) The distribution strictly obeys Loewenstein's rule, that is, the Al–Al pair avoidance rule.

The connectivity relation of the framework nodes can be uniquely represented by a connectivity matrix having 0 and 1. In a given matrix, the summation on each node in a column or a row gives 4 in number (fig. 7(a)), reflecting the number of

(a)

| node number | 1 | 2 | 3 | 4 | 5 | 6 | 7 | 8 | 9 | 10 | 11 | 12 |
|---|---|---|---|---|---|---|---|---|---|---|---|---|
| 1 | 0 | 0 | 0 | 0 | 1 | 1 | 0 | 0 | 0 | 0 | 1 | 1 |
| 2 | 0 | 0 | 0 | 1 | 0 | 1 | 0 | 0 | 0 | 1 | 0 | 1 |
| 3 | 0 | 0 | 0 | 1 | 1 | 0 | 0 | 0 | 0 | 1 | 1 | 0 |
| 4 | 0 | 1 | 1 | 0 | 0 | 0 | 0 | 1 | 1 | 0 | 0 | 0 |
| 5 | 1 | 0 | 1 | 0 | 0 | 0 | 1 | 0 | 1 | 0 | 0 | 0 |
| 6 | 1 | 1 | 0 | 0 | 0 | 0 | 1 | 1 | 0 | 0 | 0 | 0 |
| 7 | 0 | 0 | 0 | 0 | 1 | 1 | 0 | 0 | 0 | 0 | 1 | 1 |
| 8 | 0 | 0 | 0 | 1 | 0 | 1 | 0 | 0 | 0 | 1 | 0 | 1 |
| 9 | 0 | 0 | 0 | 1 | 1 | 0 | 0 | 0 | 0 | 1 | 1 | 0 |
| 0 | 0 | 1 | 1 | 0 | 0 | 0 | 0 | 1 | 9 | 0 | 0 | 0 |
| 11 | 1 | 0 | 1 | 0 | 0 | 0 | 1 | 0 | 1 | 0 | 0 | 0 |
| 12 | 1 | 1 | 0 | 0 | 0 | 0 | 1 | 1 | 0 | 0 | 0 | 0 |
| | 4 | 4 | 4 | 4 | 4 | 4 | 4 | 4 | 4 | 4 | 4 | 4 |

(b)

| node number | 1 | 2 | 3 | 4 | 5 | 6 | 7 | 8 | 9 | 10 | 11 | 12 |
|---|---|---|---|---|---|---|---|---|---|---|---|---|
| | -2 | 0 | 0 | 0 | -1 | -1 | 0 | 0 | 0 | 0 | -1 | -1 |
| | 0 | 0 | 0 | 1 | 0 | 1 | 0 | 0 | 0 | 1 | 0 | 1 |
| | 0 | 0 | -2 | -1 | -1 | 0 | 0 | 0 | 0 | -1 | -1 | 0 |
| | 0 | 1 | -1 | 0 | 0 | 0 | 0 | 1 | 1 | 0 | 0 | 0 |
| | -1 | 0 | -1 | 0 | 0 | 0 | 1 | 0 | 1 | 0 | 0 | 0 |
| | -1 | 1 | 0 | 0 | 0 | 0 | 1 | 1 | 0 | 0 | 0 | 0 |
| | 0 | 0 | 0 | 0 | 1 | 1 | 0 | 0 | 0 | 0 | 1 | 1 |
| | 0 | 0 | 0 | 1 | 0 | 1 | 0 | 0 | 0 | 1 | 0 | 1 |
| | 0 | 0 | 0 | 1 | 1 | 0 | 0 | 0 | 0 | 1 | 1 | 0 |
| | 0 | 1 | -1 | 0 | 0 | 0 | 0 | 1 | 1 | 0 | 0 | 0 |
| | -1 | 0 | -1 | 0 | 0 | 0 | 1 | 0 | 1 | 0 | 0 | 0 |
| | -1 | 1 | 0 | 0 | 0 | 0 | 1 | 1 | 0 | 0 | 0 | 0 |
| | -6 | 4 | -6 | 2 | 0 | 2 | 4 | 4 | 4 | 2 | 0 | 2 |

node index

Fig. 7. (a) Connectivity matrix, and (b) its substituted one of sodalite framework. Numerals in the lower line show the node indices.

connective bonds. However, when a given node is substituted for an Al atom, we assume the sign of the matrix elements of the reference node along both column and row is changed, and substitute the number −2 at its diagonal site; then the summation on each node gives any of six kinds of numbers, such as −6, −4, −2, 0, 2, 4 (fig. 7(b)). We call them "node indices". They are determined in terms of the connectivity relation between one centering node and its first surrounding nodes.

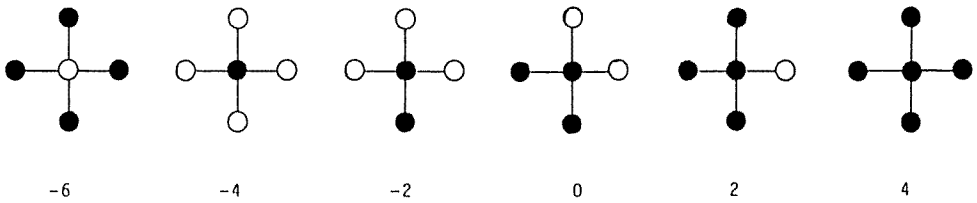


Fig. 8. Node indices and their corresponding clusters in which open circles denote Al atoms, while solid circles denote Si atoms.

As shown in fig. 8, the index 4 denotes one centering Si node to be connected with four neighboring Si nodes, the index 2 with three Si's and one Al, the index 0 with two Si's and two Al's, the index $-2$ with one Si and three Al's, the index $-4$ with four Al's, and the index $-6$ has one centering Al node to be connected with four Si nodes. It must be mentioned that in these indices, only the node having an index 4 is permitted to be replaced with Al. Otherwise, Loewenstein's rule will be violated.

The process of distribution is shown in table 1, in which a sodalite cage having 12 nodes is taken as an example. Starting with a sequence whose node indices are all numbered with 4, one Al substitution is carried out from the left-hand side to the right-hand side. The total number of one substitution sequence is 12. In the second substitution, one more Al substitution can be carried out on the one Al substitution sequence already obtained. In this case, we must select a node siting on the right-hand side of the node of index $-6$. This avoids duplication of counting. Thus, the total number of the two substitution sequences becomes 42. The procedure is continued until the node index 4 no longer occurs in the sequence. Thus, we obtain a final substitution number 6 (Si/Al = 1). This is the maximum substitution number permitted for a sodalite cage under the restriction of Loewenstein's rule. Some of the application examples for other frameworks are shown in table 2. It is noteworthy that in this distribution process, not only the total number for each substitution number, but also the maximum substitution number can be determined. For example, in the albite framework, the maximum substitution number is determined to be 6 (Si/Al = 5/3), in zeolite A to be 9 (5/3), in scapolite to be 8 (2/1), and in zeolite L to be 12 (2/1).

The distributions are obviously determined by the topological characteristics of the framework. Conversely, this means that the frameworks having the same distribution numbers and the maximum substitution number can be identified to be of the same topological characteristics.

As already stated, it is very difficult to determine the exact Al site in zeolite frameworks, both experimentally and theoretically. The method mentioned above shows all of the possible distributions, but does not indicate which distribution is actually realized; for that, an exact electrostatic potential or quantum chemical

Table 1

Distribution process of Al atoms on the node sites of a sodalite framework. Column 1 (Al no.) shows the number of Al atoms to be distributed, column 2 (*S*) the sequential number given for different Al distributions, and columns 3 to 14 give the node indices on the corresponding node sites

| Al no. | *S* | Node number | | | | | | | | | | | |
|---|---|---|---|---|---|---|---|---|---|---|---|---|---|
| | | 1 | 2 | 3 | 4 | 5 | 6 | 7 | 8 | 9 | 10 | 11 | 12 |
| 0 | 1 | 4 | 4 | 4 | 4 | 4 | 4 | 4 | 4 | 4 | 4 | 4 | 4 |
| 1 | 1 | −6 | 4 | 4 | 2 | 2 | 4 | 4 | 4 | 4 | 4 | 2 | 2 |
| | 2 | 4 | −6 | 4 | 2 | 4 | 2 | 4 | 4 | 4 | 2 | 4 | 2 |
| | 3 | 4 | 4 | −6 | 2 | 2 | 4 | 4 | 4 | 4 | 2 | 2 | 4 |
| | – | – | – | – | – | – | – | – | – | – | – | – | – |
| | 12 | 2 | 2 | 4 | 4 | 4 | 4 | 2 | 2 | 4 | 4 | 4 | −6 |
| 2 | 1 | −6 | −6 | 4 | 2 | 2 | 0 | 4 | 4 | 4 | 2 | 2 | 0 |
| | 2 | −6 | 4 | −6 | 2 | 0 | 2 | 4 | 4 | 4 | 2 | 0 | 2 |
| | 3 | −6 | 2 | 2 | −6 | 2 | 2 | 4 | 2 | 2 | 4 | 2 | 2 |
| | 4 | −6 | 4 | 4 | 4 | 0 | 0 | −6 | 4 | 4 | 4 | 0 | 0 |
| | – | – | – | – | – | – | – | – | – | – | – | – | – |
| | 42 | 0 | 2 | 2 | 4 | 4 | 4 | 0 | 2 | 2 | 4 | −6 | −6 |
| 3 | 1 | −6 | −6 | −6 | 0 | 0 | 0 | 4 | 4 | 4 | 0 | 0 | 0 |
| | 2 | −6 | −6 | 4 | 2 | 0 | −2 | −6 | 4 | 4 | 2 | 0 | −2 |
| | 3 | −6 | −6 | 4 | 0 | 2 | −2 | 4 | −6 | 4 | 0 | 2 | −2 |
| | 4 | −6 | −6 | 4 | 0 | 0 | 0 | 4 | 4 | −6 | 0 | 0 | 0 |
| | 5 | −6 | 4 | −6 | 2 | −2 | 0 | −6 | 4 | 4 | 2 | −2 | 0 |
| | – | – | – | – | – | – | – | – | – | – | – | – | – |
| | 52 | 0 | 0 | 0 | 4 | 4 | 4 | 0 | 0 | 0 | −6 | −6 | −6 |
| 6 | 1 | −6 | −6 | −6 | −4 | −4 | −4 | −6 | −6 | −6 | −4 | −4 | −4 |
| | 2 | −4 | −4 | −4 | −6 | −6 | −6 | −4 | −4 | −4 | −6 | −6 | −6 |

Table 2

Number of possible Al distributions in the restriction of Loewenstein's rule. Column 1 (Al no.) shows the number of Al atoms to be distributed, and columns 2 to 6 total numbers for different Al distributions in Sod (sodalite), alb (albite), ZTA (zeolite A), sca (scapolite), and LTL (zeolite L)

| Al no | Sod | alb | LTA | sca | LTL |
|---|---|---|---|---|---|
| 1 | 12 | 16 | 24 | 24 | 36 |
| 2 | 42 | 88 | 228 | 228 | 558 |
| 3 | 52 | 200 | 1112 | 1104 | 4896 |
| 4 | 33 | 180 | 3036 | 2936 | 26925 |
| 5 | 12 | 48 | 4776 | 4336 | 97212 |
| 6 | 2 | 8 | 4316 | 3480 | 235054 |
| 7 | | | 2184 | 1440 | 381888 |
| 8 | | | 588 | 264 | 412595 |
| 9 | | | 64 | | 288952 |
| 10 | | | | | 124944 |
| 11 | | | | | 30240 |
| 12 | | | | | 3148 |

calculation based on the three-dimensional configuration is needed. Instead of this, a simple approach is used here. In the above distribution, if Loewenstein's rule strictly holds, individual distributions can be fully expected to occur with equal probability for a given substitution number. In this condition, the summation of Al numbers on each node site gives the expected occupancy frequency at the site.

One application example for ZSM-5 will be shown here. ZSM-5 is a well-known methanol-to-gasoline conversion catalyst. ZSM-5 (space group *Pnma*) contains 96 nodes in the unit cell, as well as 12 crystallographically independent nodes. The distribution is performed on the 12 independent nodes. Table 3 shows the results,

Table 3

Predicted Al occupancy frequencies on the node sites in a ZSM-5 framework. Column 1 (Al) shows the number of Al atoms to be distributed, column 2 (Z) the total numbers for different Al distributions, and columns 3 to 14 the Al occupancy frequencies on the corresponding node sites

| Al | Z | Node number | | | | | | | | | | | |
|---|---|---|---|---|---|---|---|---|---|---|---|---|---|
| | | 1 | 2 | 3 | 4 | 5 | 6 | 7 | 8 | 9 | 10 | 11 | 12 |
| 1 | 12 | 1 | 1 | 1 | 1 | 1 | 1 | 1 | 1 | 1 | 1 | 1 | |
| 2 | 44 | 7 | 7 | 7 | 7 | 7 | 8 | 7 | 8 | 8 | 7 | 8 | |
| 3 | 58 | 13 | 14 | 13 | 13 | 14 | 13 | 18 | 12 | 17 | 17 | 12 | 18 |
| 4 | 26 | 6 | 10 | 6 | 6 | 11 | 6 | 14 | 4 | 10 | 11 | 5 | 13 |
| 5 | 2 | 0 | 2 | 0 | 0 | 2 | 0 | 2 | 0 | 1 | 1 | 0 | 2 |

in which column 1 indicates the substitution number of Al, column 2 the total number of distributions for each substitution number, and column 3 the expected occupancy frequency of Al on each node site. In the 1 and 2 substitutions, there is no distinct difference in the site occupancy, but with increasing substitution number, the difference becomes remarkable. In the case of the maximum substitution number 5, it is obvious that the node numbers 2, 5, 7 and 12 are preferentially occupied by Al atoms. Fripiat et al. [21] tried to characterize the Si, Al distribution by the SCF-MO method, and determined the preference site of Al atoms as the node numbers 2 and 12. The present result is consistent with the one by Fripiat et al. The Al preference site in the ZSM-5 framework can be represented on the Hamiltonian graph, which gives a direct measuring for topological distances between the Al nodes distributed in the framework (fig. 9).

It is now possible to derive all the Si, Al distributions in both the framework topological and Loewenstein's restrictions. Although a number of papers have been published on the Si, Al distribution in the framework which were determined by the X-ray or $^{29}$Si NMR method, it must be noted that most of them give the result averaged statistically and it is impossible to recognize their real distribution. However, if the present result is combined with experimental data, a deeper insight into the distribution will be possible. Details of this will be described in a future paper.

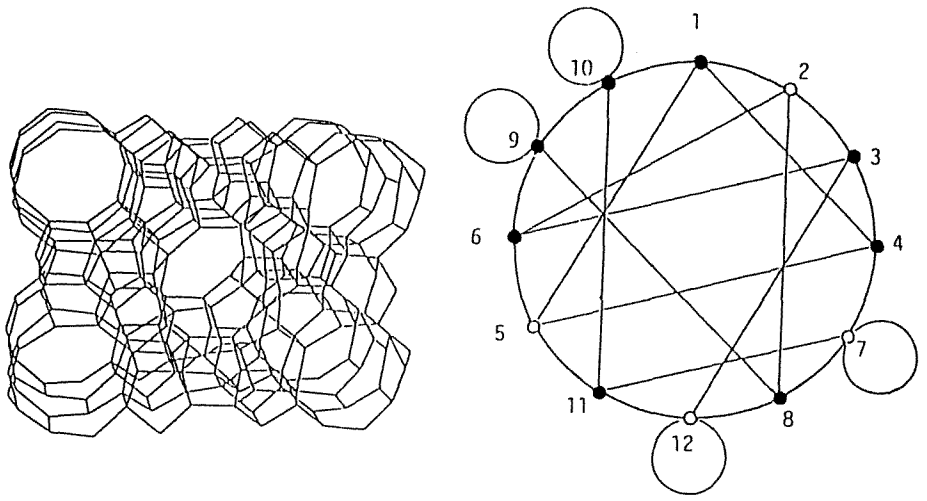


(a) (b)

Fig. 9. (a) ZSM-5 zeolite framework, and (b) its Hamiltonian graph representation, in which open circles show the predicted preference sites of Al atoms.

## Acknowledgement

I would like to thank Professor Y. Shibata, Department of Information Science, Gunma University, for his critical discussions.

## References

[1] W.M. Meier, in: *Molecular Sieves* (Soc. Chem. Ind., London, UK, 1968), p. 10.
[2] W.M. Meier, in: *Proc. 7th Int. Zeolite Conf*, Tokyo, ed. Y. Murakami, A. Iizima and J.W. Ward (Kodansha, Elsevier, Japan, 1986), p. 13.
[3] M. Sato, J. Phys. Chem. 91(1987)4675.
[4] W.M. Meier and H.J. Moeck, J. Sol. State Chem. 27(1979)349.
[5] W.M. Meier and D.H. Olson, *Atlas of Zeolite Structure Types*, 2nd ed. (International Zeolite Association, Butterworths, USA, 1987).
[6] M. Sato and T. Ogura, Chem. Lett. (1980)1381.
[7] M. Sato, *Proc. 6th Int. Zeolite Conf.*, Reno, ed. D. Olson and A. Bisio (Butterworths, UK, 1983), p. 851.
[8] F. Harary, *Graph Theory* (Addison–Wesley, 1972).
[9] G. von Engelhardt, U. Louse, E. Lippma, M. Tarmak and M. Magi, Z. Anorg. Allg. Chem. 482(1981)49.
[10] S. Ramdas, J.M. Thomas, J. Klinowski, C.A. Fyfe and J.S. Hartman, Nature 292(1981)228.
[11] M.T. Melchior, D.E.W. Vaughan and A.J. Jacobson, J. Amer. Chem. Soc. 104(1982)4859.
[12] A.W. Peters, J. Phys. Chem. 86(1982)3489.
[13] J. Klinowski, S. Ramdas, J.M. Thomas, C.A. Fyfe and J.S. Hartman, J. Chem. Soc. Faraday Trans. 2, 78(1982)1025.
[14] B. Beagly, J. Dwyer, F.R. Fitch, R. Mann and J. Walters, J. Phys. Chem. 88(1984)1744.

[15] A.J. Vega, in: *Intrazeolite Chemistry* (ACS Symposium Series 218), ed. G.D. Stucky and F.G. Dwyer (Americal Chemical Society, 1983), p. 217.
[16] M.T. Melchior, *Intrazeolite Chemistry* (ACS Symposium Series 218), ed. G.D. Stucky and F.G. Dwyer (Americal Chemical Society, 1983), p. 243.
[17] S. Beran and J. Dubsky, J. Phys. Chem. 83(1979)2538.
[18] W.J. Mortier and P. Geering, J. Phys. Chem. 84(1980)1982.
[19] S. Beran, Z. Phys. Chem. 123(1980)129.
[20] E.C. Hass and P.G. Mezey, J. Mol. Struct. 87(1982)261.
[21] J.G. Fripiat, F. Berger-Andre, J.-M. Andre and E.G. Derouane, Zeolites 3(1983)306.
[22] S. Beran, Z. Phys. Chem. 137(1983)89.
[23] J.G. Fripiat, P. Galet, J. Delhalle, J.M. Andre, J.B. Nagy and E.G. Derouane, J. Phys. Chem. 89(1985)1932.
[24] E.G. Derouane and J.G. Fripiat, Zeolites 5(1985)165.